

# Simulation of Field Model Tests by two different Numerical Approaches

*Urs Vogler  
Corne J. Coetzee  
Pieter A. Vermeer*

## 1. Introduction

Geotechnical engineers are often confronted with complex soil profiles and limited field data. As a consequence predictions of load-settlement curves are difficult, at least as long as the computational model is not calibrated by in situ testing. For testing and validating the performance of constitutive models and numerical procedures, it is therefore desirable to consider relatively simple model tests on homogeneous subsoil. In Stuttgart such tests were carried out by Rilling (1994) on a clayey silt; a classical strip footing on a half plane and a strip footing next to a vertical cut. Both field model tests are extremely well documented and the clayey silt was extensively tested in the lab. Unfortunately measured triaxial curves were partly lost, but shear strength data were fully available.

Although both tests involve plane strain strip footings on the same type of soil, they are completely different. The footing near the vertical cut involves a collapse mechanism as considered in slope stability analyses and the other one yields a Prandl-type failure. This is also reflected in the magnitudes of the collapse loads, being very low for the slope-type failure and high for the usual bearing capacity problem. Considering these different stress levels and different collapse mechanisms, these field model tests are outstanding for validating numerical collapse load calculations. Numerical collapse load analyses are not directly needed for simple situations such as a footing on a homogeneous half space, as this bearing capacity problem has been solved analytically, but it is essential for more complex problems, e.g. for a footing near a slope as also considered in this study.

In the present paper all collapse load calculations will be based on the conventional Mohr-Coulomb failure criterion, which incorporates the same friction angle both for standard triaxial conditions and for plane-strain conditions. Laboratory tests have shown that this is not the case and researchers like Wroth (1984) and others have suggested that the plane-strain friction angle is about 10 percent larger than the triaxial one. Nevertheless we will initially use the triaxial friction angle and cohesion as observed in triaxial tests. On comparing computed collapse loads, it will then be concluded that the plane-strain friction angle is indeed 10 percent larger than the triaxial friction angle.

As lab testing data on the soil stiffness were not available, we have used the simple Mohr-Coulomb model in combination with curve fitting for the stiffness. Hence, the MC-model is not chosen because we think that this constitutive model is suitable for settlement predictions, but because data for proper settlement predictions were not available. On the other hand, perfect-plasticity models are appropriate for collapse load analyses, as shown by Vermeer et al. (2002) for face stability of tunnels and as will be shown in this study for strip footings.

Calculations will be carried out by two basically different methods, i.e. a more or less conventional nonlinear, elastoplastic finite element method and a recently developed alternative, being referred to as the Material Point method. The latter method will be briefly explained as this one is hardly known in geotechnical engineering.

## 2. Field Tests and Soil Parameters

Large scale field tests (experiments) were performed by Rilling 1994 to investigate bearing capacity and slope stability problems.

### 2.1. Test Setup

The frame depicted in Fig. 1 was used to perform tests under plane strain conditions. In order to ensure plane strain on a middle section, the strip footing was divided into three parts; the outer parts were one metre long and the middle part 0.4 metre. Measurements were only done on the middle section. The sections were placed close together, but without contact. The loading was done load controlled by hydraulic presses and controlled in such a way that all three sections had the same vertical displacements. With measurements made only on the middle section, plane strain conditions (measurements) can be assumed. Fig. 2 shows typically measured load-settlement curves. This graph clearly indicates the different stress levels present in the two different problems being analysed. During the slope stability test, test A, the loading pressure is in the order of  $150 \text{ kN/m}^2$ , while during the bearing capacity test, tests B1 and B2, it is in the order of  $800\text{-}1000 \text{ kN/m}^2$ . The difference between the two B-tests, B1 and B2, is due to different locations and soil heterogeneity.

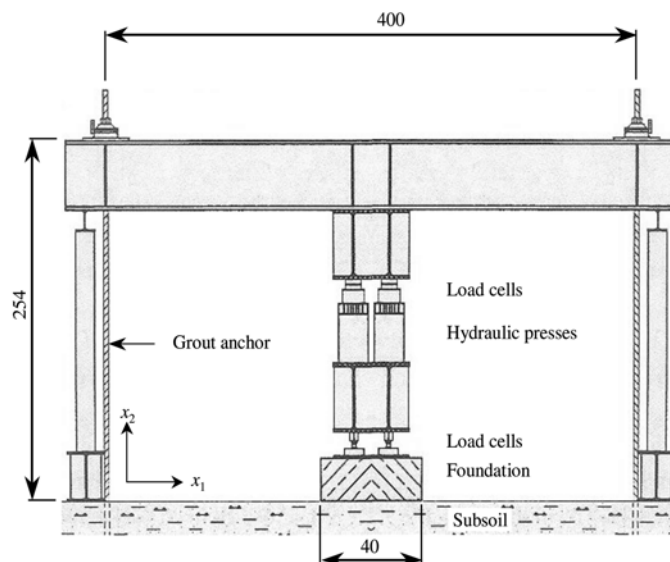


Figure 1: Test setup for performed field tests.

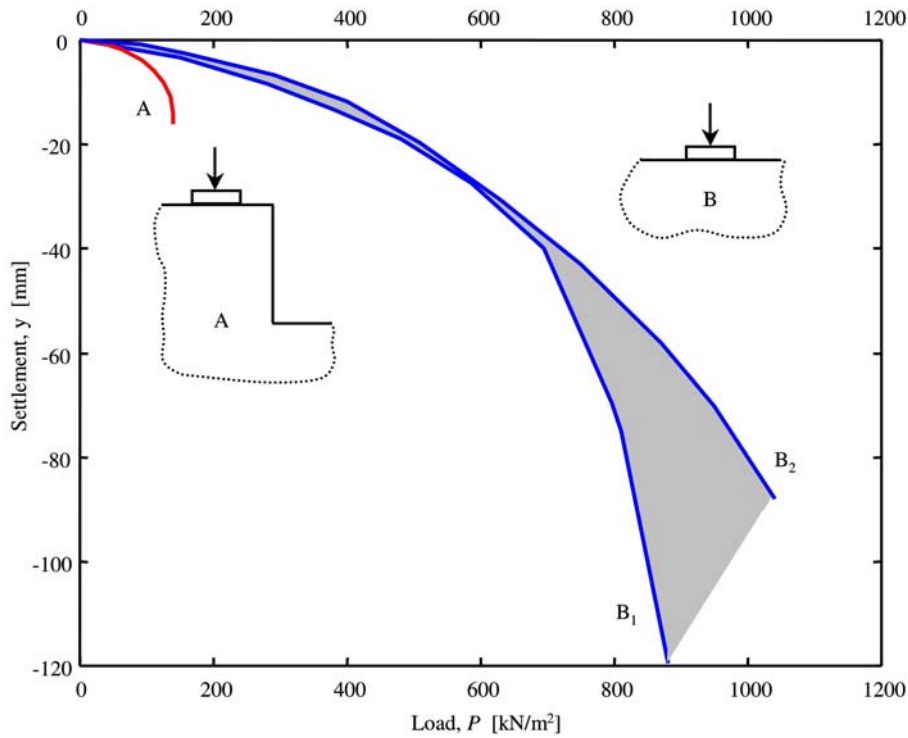


Figure 2: Load-displacement curves from field test.

## 2.2. Soil Parameters

The tests were performed on a clayey silt near the city of Heilbronn in southern Germany. The soil consists for about 70% out of quartz, 15% of feldspar and 15% of calcite, but field heterogeneity caused considerable variations about these mean values. The soil has a field porosity of about  $n = 35\%$  with  $n_{\text{water}} \approx 30\%$  and  $n_{\text{air}}$  about 5%. This gives a unit soil weight of  $\gamma = 20.5 \text{ kN/m}^3$ . The Heilbronn silt is a stiff silt with a plasticity index of  $I_p = 20\%$ . Finally it should be noted that we consider a so-called man-made soil that was deposited in layers of 35 cm and then compacted to a thickness of 25 cm.

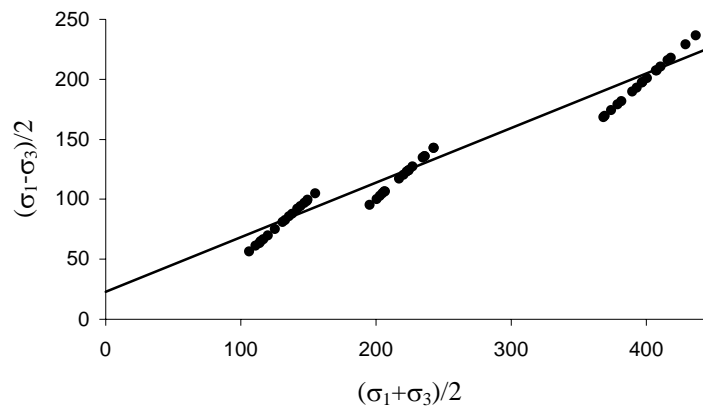


Figure 3: Triaxial results plotted the Mohr-Coulomb failure line.

Triaxial tests were carried out on soil samples taken from the artificially compacted test site. Fig. 3 shows the results from 16 different tests. Confining pressures of 50, 100 and 200 kPa were used. The friction angle and cohesion were obtained by fitting the straight line shown in the figure to the data points using linear regression. They are found to be  $c' = 26$  kPa and  $\phi' = 27^\circ$ . No consistent data on the soil stiffness is given by Rilling 1994, therefore the stiffness used in the numerical modelling was obtained by curve-fitting. Load-displacement curves for different stiffness values were compared to the measured curve, and a stiffness of  $E = 25$  MN/m<sup>2</sup> was chosen for use in an elastic perfectly plastic Mohr-Coulomb model. All soil data is assembled in table 1.

Table 1: Heilbronn silt parameters

Young's modulus, E [kN/m <sup>2</sup> ]	25 000
Unit soil weight, $\gamma$ [kN/m <sup>3</sup> ]	20.5
Poisson's ratio, $\nu$ [-]	1/3
Cohesion, $c'$ [kPa]	26
Dilatancy, $\psi$ [°]	0
Friction, $\phi'$ [°]	27

### 3. The Material-Point Method

In many engineering problems such as silo discharging and earth moving processes, large displacements occur. When these problems are modeled by a usual Lagrangian finite element method, the mesh becomes so distorted that remeshing is needed. During the remeshing process stresses and strains have to be mapped from the distorted mesh to the newly defined mesh, which introduces difficulties. Therefore researchers have worked on new finite element methods for which the large-displacement solution is not so mesh-dependent. In the early nineties such new FE-methods were introduced into solid mechanics under the name meshless methods. This name is deceiving as one does use a mesh. However the mesh does not deform. Instead a so-called Eulerian FE-method is used, in which material points are moving through a fixed mesh, so that there will never be any mesh distortion.

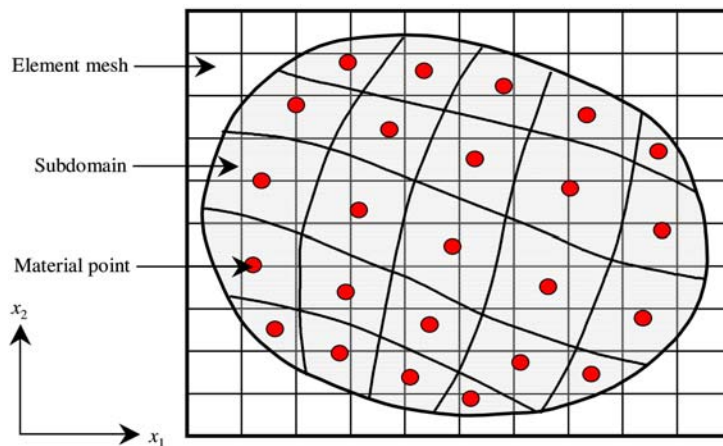


Figure 4: The element mesh and material points within the sub domains

In this paper we will use a so-called “meshless” method, or rather Eulerian FE-method, being referred to as Material Point method. A variation of this method has been described by Burgess et al. (1992) and Sulsky and Schreyer (1993, 1996). They showed the capacity of this method for the analysis of dynamic impact and penetration. Most recently Wieckowsky (1999, 2002) applied the method to silo discharging although the Material Point method is tailor-made for very large displacements. Attention will be focused on strip footing problems, in which displacements remain relatively small. On choosing such problems, results of the new Material Point method can be compared to results of a conventional Lagrangian FEM.

In the following we will give a very brief outline of the method. First a finite element mesh is introduced. For the present analyses, we will use a regular grid of 4-noded quadrilateral elements as indicated in Fig. 2. This grid may extend well beyond the soil body to be considered. The initial configuration of the soil body is now divided into a large number of small subregions. In general a quadrilateral 4-noded element is considered an initial subregion, but the initial subregions may also deviate from the quadrilaterals, as indicated in Fig. 4. In the center of each subregion a material point is placed, which represents the subregion. Non-linear deformation problems are solved stepwise, as in a classical FE-analysis, but instead of updating the position of the mesh nodes after each step, one will only update the position of the material points. These points will thus move away from their initial position on the center of a 4-noded quadrilateral. Likewise the subdomains that are represented by the material points will also become independent from the finite element grid as indicated in Fig. 4.

The Material Point method as programmed by Coetzee is a dynamic finite element code in which inertia effects are fully taken into account. For quasi-static problems, as considered in this study, one simply introduces a low rate of footing indentation so that inertia effects become small. The programming by Coetzee involves a so-called explicit time integration, which requires very small time steps. In contrast the PLAXIS finite element code is based on implicit integration of the differential constitutive law, so that accuracy is even retained for relatively large loading steps.

It may thus be concluded that the two methods are basically different and it will be interesting to see whether or not they produce the same results.

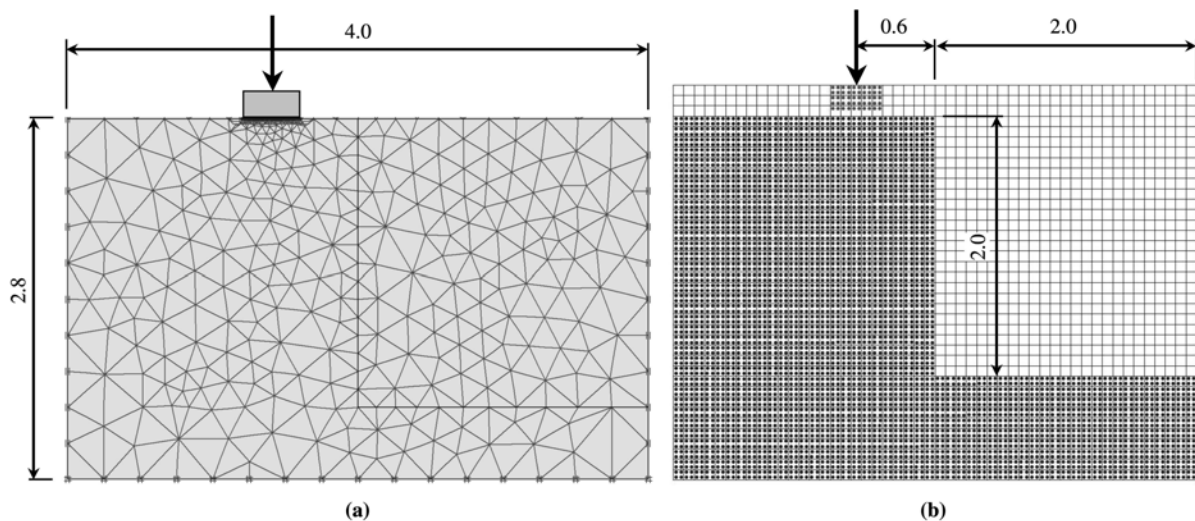


Figure 5: Discretisation of strip footing problem A. FE-mesh for PLAXIS to the left and grid for Material Point method to the right.

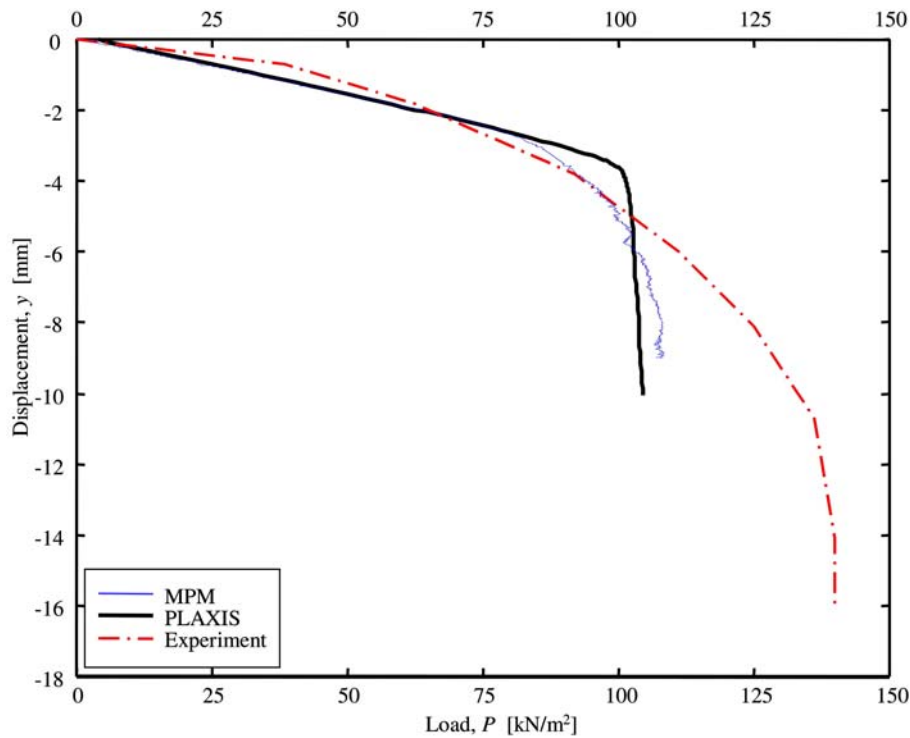


Figure 6: Load-displacement curves for strip footing A.

#### 4.1 Strip Footing Problem A

Fig. 5 shows the meshes that were used to model the strip footing problem A. In PLAXIS a total of 774 6-noded elements were used with 1664 nodes. In the Material Point analysis a regular grid of  $50 \times 35 = 1750$  square 4-noded elements was used with a total of 1836 nodes. The left side boundary was assumed smooth, i.e., only constrained in the horizontal direction. The bottom boundary was constrained in both the horizontal and vertical directions. The initial stress state was generated by first creating material over the whole domain, using  $K_0 = 1 - \sin\phi'$ . The vertical cut was then generated by removing the material layer by layer. After each removal, the material was allowed to deform and to reach static equilibrium. Fig. 6 shows the load-settlement curves for this problem. The MP and PLAXIS results are in good agreement, but underestimate the failure load by roughly 30 percent. For details the reader is referred to Vogler (2001).

#### 4.2 Strip Footing Problem B

Fig. 7 shows the meshes that were used to model the strip footing problem B. In PLAXIS a total of 1050 6-noded elements were used with 2171 nodes. In the Material Point method a regular grid of  $45 \times 30 = 1350$  square 4-noded elements was used with a total of 1426 nodes. Despite the comparable number of nodes the MP-grid is finer than the PLAXIS mesh, as the MP-analysis was carried out for half a symmetric footing. The side boundaries were assumed smooth, i.e., only constrained in the horizontal direction. The bottom boundary was constrained in both the horizontal and vertical directions. A  $K_0 = 1 - \sin\phi'$  initial stress state was assumed.

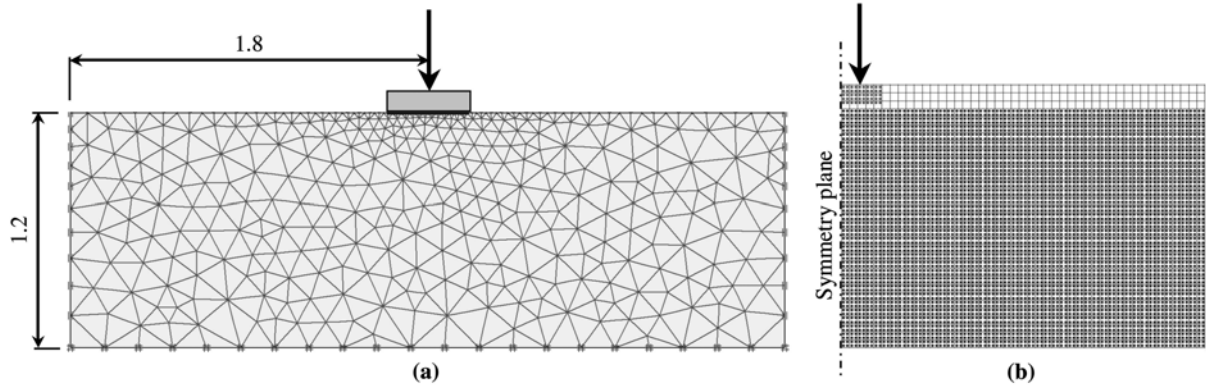


Figure 7: Discretisation of strip footing problem B. FE-mesh for PLAXIS to the left and grid for Material Point method to the right.

Fig 8 shows the load-settlement curves obtained from field measurements and using MPM and PLAXIS. There is a good correspondence between the MPM and PLAXIS results, predicting failure loads of 692 and 668 kN/m<sup>2</sup> respectively. The numerical methods accurately predict the measured initial stiffness and corresponds well to the field data up until the predicted failure loads are reached. The failure load, however, is underestimated by approximately 25%. This difference might be due to several factors, as will be discussed later.

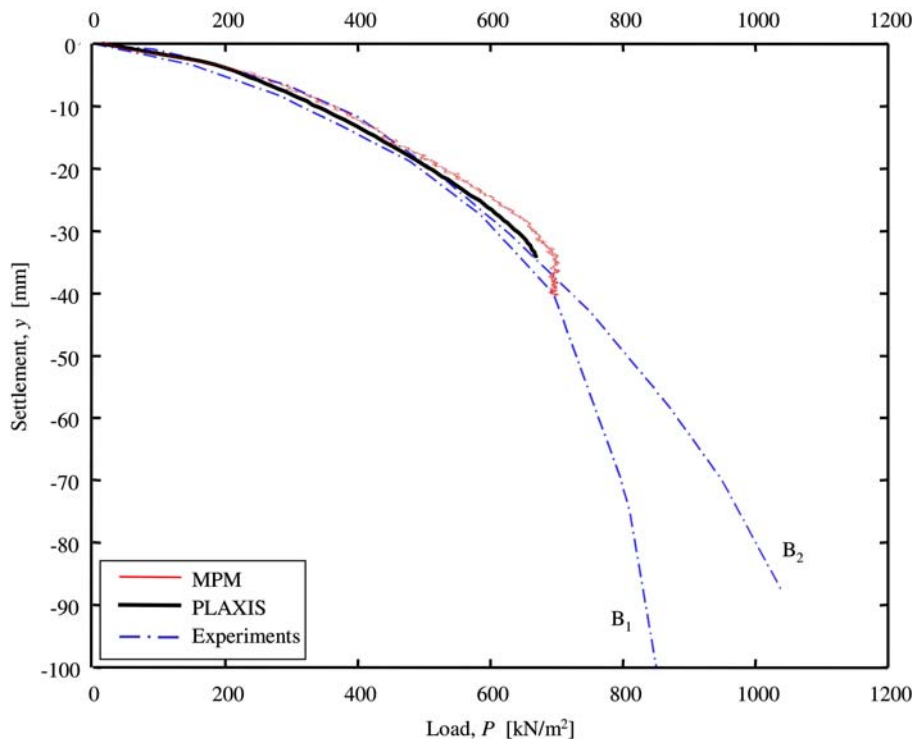


Figure 8: Load-displacement curves for strip footing B

## 5. Concluding Remarks.

This study leads first of all to the conclusions that the new Material Point method produces results that coincide more or less to the ones from a conventional nonlinear elastoplastic FE-method. For small-strain deformation problems, the conventional FE-analysis would seem to be the most appropriate method as it is much more easy to apply than the MP-method, but the latter would seem to be most convenient for large-deformation problems. Indeed, the MP-method overcomes the drawback of classical FE-methods that large deformations result in severe mesh distortions.

Experiences with strip footing analyses have learned that numerical procedures often become unstable when failure approaches. Such difficulties were now primarily encountered for footing B. It is striking that numerical instability was both observed for the classical FEM and for the new Material Point method, although both methods involve completely different numerical procedures. Indeed, the classical FEM is a so-called implicit method with static equilibrium iterations, whereas the MP-method is applied in combination with a pseudo-dynamic explicit solution procedure. As both methods turned out to be unstable upon reaching the collapse load, it would seem that problem B is intrinsically unstable, even in combination with displacement control.

Another observation is that the failure load is significantly underestimated by both numerical analyses. In order to understand this fact one might consider the analytical solution of Soil Mechanics text books, which reads

$$\begin{aligned} P_{\max} &= c' \cdot N_c + \gamma \cdot b \cdot N_b & , & \quad N_c = \frac{N_d - 1}{\tan \varphi'} \\ N_b &= (N_d - 1) \cdot \tan \varphi' & , & \quad N_d = \frac{1 + \sin \varphi'}{1 - \sin \varphi'} \cdot e^{\pi \cdot \tan \varphi'} \end{aligned}$$

where  $b$  is the width of the footing. On evaluating the analytical solution it is found for strip footing B that

$$P_{\max} = 26 \cdot 24 + 20.5 \cdot 0.4 \cdot 62 = 623 + 51 = 674 \text{ kPa}$$

where  $N_c$  and  $N_b$  are updated for  $\varphi' = \varphi'_{tr} = 27^\circ$  obtained from triaxial testing data. The value of 674 kPa corresponds well to the numerical results, but not to the measured values. In order to match the latter values, one would have to use a friction angle of  $\varphi' = \varphi'_{ps} = 30^\circ$  which would yield  $P_{\max} = 946 \text{ kPa}$ . Hence we should not have chosen the triaxial compression angle of  $\varphi'_{tr} = 27^\circ$ , but a slightly larger plane-strain friction angle of  $\varphi'_{ps} = 30^\circ$ . Our numerical analyses simply show that  $\varphi'_{ps} / \varphi'_{tr} = 1.1$ . For cohesive soils, this ratio of 1.1 is also suggested by Kulhawy and Mayne (1990), whilst Wroth (1984) suggested the very similar ratio of 9 / 8. Indeed, triaxial compression tests give relatively low friction angles and the use of such values in computations is conservative. For Geotechnical design, it may be right to chose conservative values, but this should not be done when numerical analyses are used to predict reality.

## Bibliography

- [1] Rilling, B. Untersuchungen zur Grenztragfähigkeit bindiger Schüttstoffe am Beispiel von Lösslehm. Phd Thesis, Institute for Geotechnical Engineering, University of Stuttgart, 1994.
- [2] Wroth, C.P., Interpretation of In-Situ Soil Tests. *Geotechnique*, Vol. 34, No. 4, Dec. 1984, 449--489
- [3] Vermeer, P.A., Ruse, N., Marcher, T. Tunnel Heading Stability in Drained Ground. *Felsbau*, Jg. 20.2002, No. 6, 8--18.
- [4] Vermeer, P.A. Marcher, T., Ruse, N. On the Ground Response Curve. *Felsbau*, Jg. 20.2002, NO. 6, 19--24.
- [5] Burgess, D., Sulsky, D., Brackbill, JU. Mass matrix formulation of the FLIP particle-in-cell method. *Journal of Computational Physics*, 1992; 103, 1--15.
- [6] Sulsky, D., Schreyer, HL. Axisymmetric form of the material point method with application to upsetting and taylor impact problems. *Computer Methods in Applied Mechanics and Engineering* 1996; 139, 409--429.
- [7] Sulsky, D., Schreyer, HL. A particle method with large rotations applied to the penetration of history-dependent materials. *Advances in Numerical Simulation Techniques for Penetration and Perforation of Solids*, ASME, AMD 1993; 171, 95--102.
- [8] Wieckowski, Z., Youn, S.-K., Yeon, J.-H. A Particle-in-Cell solution to the silo discharging problem. *Int. J. Numer. Meth. Engng* 1999; 45, 1203--1225.
- [9] Wieckowski, Z. Analysis of granular flow by the material point method. Fifth World Congress on Computational Mechanics WCCM V, Mang HA, Rammerstorfer FG, Eberhardsteiner J, (eds). July 7-12, 2002, Vienna, Austria.
- [10] PLAXIS Finite element code for soil and rock analyses. Balkema, Rotterdam. \ \ <http://www.plaxis.com> [2 June 2003].
- [11] Vogler, U. Zur numerischen Untersuchung der Grenztragfähigkeit von Lößlehm. Institute of Geotechnical Engineering, University of Stuttgart, Diploma thesis 115, 2001.
- [12] Kulhawy, F.H., Mayne, P.W. Manual on Estimating Soil Properties for Foundation Design. Final Report, 1990.

**Anschrift des Verfassers:** Dipl.-Ing. Urs Vogler  
Universität Stuttgart  
Fakultät Bauingenieurwesen  
Institut für Geotechnik  
Pfaffenwaldring 35  
D-70569 Stuttgart